Journal Name RSCPublishing

COMMUNICATION

Cite this: DOI: 10.1039/x0xx00000x

Epitaxial antiperovskite superconducting $CuNNi_3$ thin films by chemical solution deposition†

Zhenzhen Hui,[a‡] Xianwu Tang,[a‡] Dingfu Shao,[a] Hechang Lei,[a] Jie Yang,[a] Wenhai Song,[a] Hongmei Luo,[b] Xuebin Zhu[*a] and Yuping Sun[*ac]

Received 00th xxxxxxx 201x, Accepted 00th xxxxxxx 201x

DOI: 10.1039/x0xx00000x

www.rsc.org/

Epitaxial antiperovskite superconducting $CuNNi_3$ thin films have been grown by chemical solution deposition. The film is a type II superconductor and shows a T_c of 3.2 K with a transition of 0.13 K. The $H_{c2}(0)$ and ξ_0 are estimated as 8.1 kOe and 201 Å, respectively.

Transition-metal nitrides and carbides have been known to exhibit lots of very important properties such as superconductivity, catalytic activity, unusual magnetic properties, and high hardness and mechanical strength.[1-3] As one typical type of transition-metal nitrides and carbides, antiperovskite structured materials have been studied intensively both by experimental and theoretical methods due to their rich physical properties as well as potential applications. Novel interesting properties, such as superconductivity in $MgCNi_3$ and $SrPPt_3$,[4,5] excellent magnetism in $RhNFe_3$,[6] giant negative thermal expansion in $Cu_{1-x}Ge_xNMn_3$,[7] have been investigated widely. However, the intrinsic physical properties have not yet been well-studied because of the challenges in preparing antiperovskite single crystals as well as in preparing high-quality antiperovskite thin films.[8] As for the antiperovskite superconducting materials, till now, to the best of our knowledge, only polycrystalline $MgCNi_3$ thin films can be successfully obtained by electron-beam evaporation[9] and there has no report about epitaxial growth of the antiperovskite superconducting thin films. In spite of a large amount of ferromagnetic Ni atoms in its unit cell, the nickel-based antiperovskite materials show superconductivity rather than magnetism. According to band-structure calculations, $MgCNi_3$ is near a ferromagnetic instability due to the high density of states at the Fermi level.[10,11] To investigate intrinsic superconducting properties, it is desirable to develop an effective route to synthesis epitaxial antiperovskite superconducting thin films. Chemical solution deposition method is an effective method with advantages of low-cost, easy set-up, coating of large areas.[12-15] However, it has never been tried to prepare antiperovskite thin films by chemical solution deposition methods. The development of an alternative synthesis route to prepare antiperovskite thin films is clearly technologically relevant to advance antiperovskite materials.

Here, we report the preparation of epitaxial superconducting antiperovskite $CuNNi_3$ (CNN) thin films on $LaAlO_3$ (LAO) substrates by chemical solution deposition. Thin films were annealed at 600 ºC for 2 hours in air and nitrogenised at 600 ºC for 2 hours under flowing ammonia atmosphere with 1 atm pressure (see electronic supplementary information (ESI), where the details of experimental procedures, characterization and theoretical calculations are presented). Recently, CNN ceramic was reported as a superconductor with a superconducting temperature T_c of 3.2 K and its structure is cubic antiperovskite with the lattice constant of 3.742 Å as shown in the inset of Figure 1a.[16] The successful growth of phase pure antiperovskite CNN thin films by a controllable and reproducible synthesis route makes it possible to study the fundamental physical properties. This achievement is also a tremendous leap toward the utilization of chemical solution methods to prepare other novel antiperovskite thin films.

Epitaxial growth of CNN thin film on LAO has been confirmed by X-ray diffraction (XRD). As shown in Figure 1a, the presence of only (002) peak from CNN indicates that the film is preferentially oriented along the c-axis. No detectable diffraction from undesirable phases such as Ni and Ni_4N suggests the formation of phase pure CNN. As shown in Figure 1b of the ϕ-scans of CNN (110) and LAO (110) reflections, four peaks with 90° apart confirm the formation of cubic CNN thin films, which are corresponding to the LAO peaks, suggesting the cube-on-cube growth mode. The epitaxial relationships between CNN and LAO are determined to be (00l)CNN//(001)LAO and [110]CNN//[110]LAO. The lattice parameter of the CNN, calculated from the (002) peak, is as a= 3.75 Å, which is same as that of the bulk CNN ceramic.[16] The lattice constant is also calculated by first-principles density functional theory (DFT) using the projected augmented-wave (PAW) method with the generalized gradient approximation (GGA) as implemented in the ABINIT code (see ESI for details). It is found that the lattice constant is decreased with decreasing N content and the lattice of the stoichiometric CNN is calculated as 3.76 Å, which is in very good agreement with the experimental result (a= 3.75 Å), indicating the stoichiometry of the derived epitaxial CNN thin film.

Microstructure and thickness of the derived CNN thin film are investigated by a field-emission scanning electron microscopy (FE-SEM). As shown in Figure 2a, it is seen that the CNN film is relatively dense without obvious porosity. The thickness measured by a cross-sectional FE-SEM is determined as 90 nm as shown in the inset of Figure 2a. To confirm the lattice constant by XRD, the lattice constant is also measured by transmission electron microscopy (TEM) as shown in Figure 2b. It is determined that the lattice constant is of 3.75 Å both from the lattice stripes and the selected area electron diffraction (SAED), which is same as the result from the XRD pattern. The stoichiometry of the CNN thin film is determined by the electron dispersion spectrum (EDS). Due to the relatively large uncertain for light elements in EDS, [17] we just give the atomic ratio of Cu: Ni, and the value is of 1: 3.03 suggesting the stoichiometry for the derived CNN thin film.

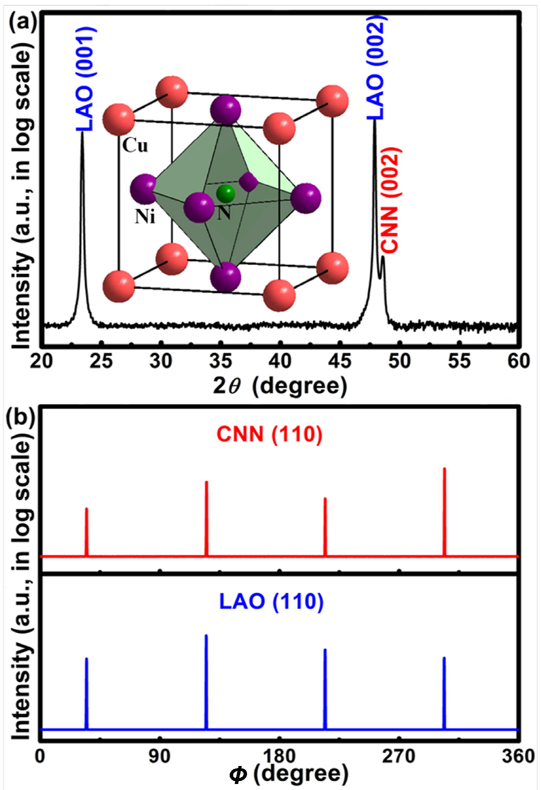

Fig. 1 (a) XRD θ-2θ result of CNN film on LAO (001) and the inset shows the crystal structure of CNN; (b) XRD ϕ-scans from (110) reflections of CNN and LAO.

Epitaxial CNN thin films exhibit different properties as compared to those of the bulk CNN ceramic. Figure 3a shows the temperature dependence of resistivity for the derived CNN thin film. The CNN thin film shows a characteristic of metallic-like resistivity-temperature above the superconducting transition. The resistivity at 300 K is 63.1 μΩ cm, which is about 5 times lower than that of the bulk CNN ceramic due to the decreased grain boundary scattering of carriers for epitaxial growth.[16] The onset superconductivity takes place at T_c of 3.2 K (at which the resistivity deviates from the normal state resistivity) and the transition width ΔT is 0.13 K (between the 90% and 10% of the normal state resistivity) as shown in the inset of Figure 3a, which are similar to the previous reports about bulk CNN ceramic.[16] Such a sharp transition indicates the high purity and high quality of the epitaxial CNN thin film. The normal state resistivity is fitted by different mechanisms. It is found that the resistivity at high temperature (50 K <T< 350 K) can be well fitted by the Bloch-Grüneisen expression[18] $\rho^{-1} = \rho_p^{-1} + (\rho_0 + \rho_{ph})^{-1}$ in the case of Einstein phonon distribution as shown in Figure 3a, with $\rho_{ph} = \rho_l \coth(\frac{\Theta_E}{2T})[1 + (\frac{2}{3})\sinh^2(\frac{\Theta_E}{2T})]^{-1}$, and Θ_E, ρ_0, ρ_p and ρ_l are, respectively, Einstein temperature, residual resistivity, parallel resistivity and a constant. The best fitting result gives Θ_E= 180.1 K, ρ_0= 8.831 μΩ cm, ρ_p= 212.1 μΩ cm and ρ_l= 25.1 μΩ cm. The Einstein temperature Θ_E is comparable with that of $MgCNi_3$ (Θ_E= 206.1 K).[19] The low temperature resistivity (5 K <T< 50 K) gives a power law, $\rho = \rho_0^* + aT^n$ and the fitting result gives ρ_0^* = 3.741 μΩ cm and n= 2.351, which is also shown in Figure 3a. The fitting results indicate that the electron-phonon scattering is the main contribution to the resistivity at high temperatures, and both the electron-phonon scattering and electron-electron scattering contribute simultaneously to the resistivity at low temperatures.[20,21] According to the theoretical calculated results (see ESI), similar to the case of $MgCNi_3$,[10,11] there is a large density of states (DOS) at E_F (N(E_F)) in CNN. From the BCS theory, a large N(E_F) can lead to a strong electron-phonon coupling.

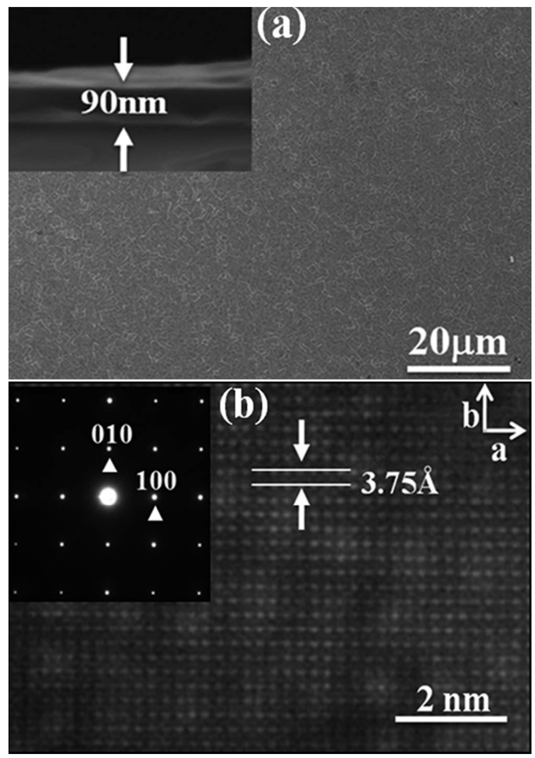

Fig. 2 (a) Surface FE-SEM result of CNN/LAO and the inset gives the thickness about 90 nm; (b) surface HRTEM result of the CNN film and the inset is the SAED.

Upper critical field (H_{c2}, the field at which a superconductor becomes normal) is a very important parameter for a superconductor. In order to determine the H_{c2}, the superconducting transition was measured as a function of magnetic fields as shown in Figure 3b. The inset of Figure 3b shows the H_{c2} corresponding to the temperatures where the resistivity drops to 50% of the normal state resistivity. According to the conventional one-band Werthamer-Helfand-Hohenberg (WHH) theory,[22] which describes the orbital limited H_{c2} of a dirty type-II superconductor, H_{c2} is described by

$H_{c2}(0) = -0.693(\frac{dH_{c2}}{dT})_{T_c} T_c$, where $H_{c2}(0)$ is the upper critical field at zero temperature. The fitting curve by the WHH theory is also shown in the inset of Figure 3b, giving the $H_{c2}(0)$ of 8.1 kOe. The superconducting coherence at zero temperature ξ_0 is estimated using the Ginzburg-Landau (GL) expression[23] $H_{c2}(0) = \Phi_0 / 2\pi\xi_0^2$ with $\Phi_0 = 2.07 \times 10^{-15} Wb$, giving the ξ_0 of 201.1 Å. The decreased $H_{c2}(0)$ as compared to that of the bulk CNN ceramic ($H_{c2}(0)$= 1.21 T),[16] suggests that there are less vortex pinning centres in epitaxial CNN thin films due to the reduced defects such as grain boundaries.

To further confirm the superconducting properties of the epitaxial CNN thin films, the temperature dependence of magnetization both FC (field-cooled) and ZFC (zero-field-cooled) protocol under an applied magnetic field of 10 Oe parallel to the film surface of the epitaxial CNN thin film were measured and the results are shown in Figure 4a. The film shows a superconducting onset of 3.15 K in terms of FC and ZFC bifurcation, which is self-consistent with the T_c determined from the resistivity, further confirming the superconducting characteristic of the epitaxial CNN thin film. There is an evidence for flux trapping too. The magnetic hysteresis loop *M(H)* at 2 K as shown in Figure 4b clearly indicates that the CNN film is a type II superconductor. The low critical field at 2 K $H_{c1}(2\ K)$ is determined as ~ 40 Oe from the low field *M(H)* at 2 K as shown in the inset of Figure 4b, by a linear fitting of the *M(H)* curve at low field, which is same as the previous report about CNN ceramic.[16]

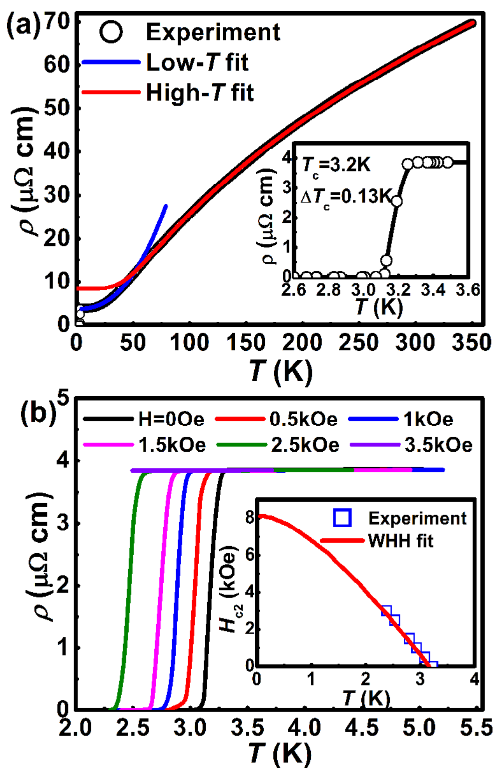

Fig. 3 (a) Temperature dependence of resistivity of the CNN film on LAO (001) under a zero field as well as the transport fitting results and the inset is the enlarged image to give a clear superconducting transition; (b) superconducting transition under different magnetic fields and the inset is the fitting result by the WHH expression.

In summary, high-quality epitaxial antiperovskite $CuNNi_3$ thin films have been synthesized by a chemical solution deposition method. The epitaxial $CuNNi_3$ thin film shows a superconducting transition of 3.2 K with a transition width of 0.13 K, a $H_{c2}(0)$ of 8.1 kOe, a ξ_0 of 201 Å. The high temperature resistivity is mainly dominated by the electron-phonon scattering and the resistivity at low temperatures is controlled by both the electron-phonon and the electron-electron scattering. The reported chemical solution deposition of epitaxial antiperovskite $CuNNi_3$ thin films will enable widely fundamental investigation about the properties as well as provide a very simple and low-cost method to prepare other epitaxial antiperovskite thin films.

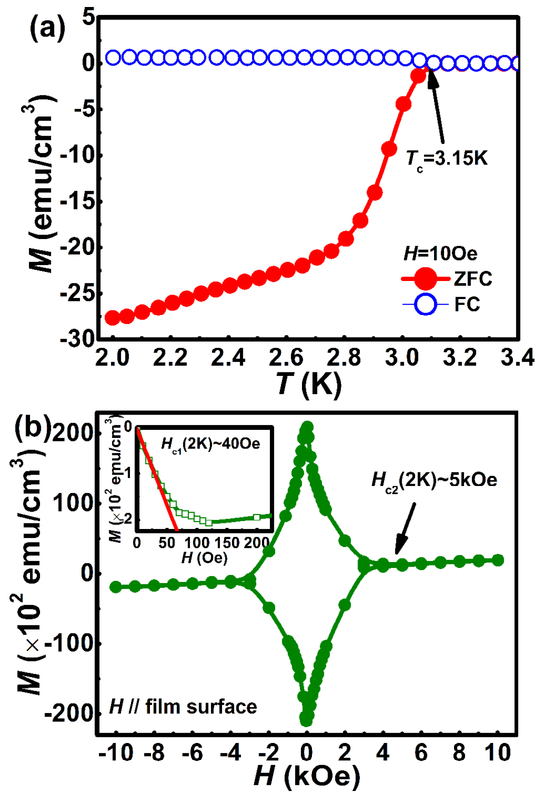

Fig. 4 (a) Temperature dependence of magnetism with FC and ZFC modes under 10 Oe applied magnetic field parallel to the surface; (b) *M(H)* loop at 2 K and the inset is the low-field *M(H)* to give the H_{c1} at 2 K.

This work was supported by the National Basic Research Program of China (2014CB931704 and 2011CBA00111) and by the National Nature Science Foundation of China under Contract Nos. 51171177 and 11174288. H. Luo acknowledges the funding support from NSF under Grant No. 1131290.

Notes and references

[a] Key Laboratory of Materials Physics, Institute of Solid State Physics, Chinese Academy of Sciences, Hefei 230031, China.
‡ These two authors contribute equally
* E-mail: xbzhu@issp.ac.cn, ypsun@issp.ac.cn
[b] Department of Chemical Engineering, New Mexico State University, Las Cruces, New Mexico 88003, USA.
[c] High Magnetic Field Laboratory, Chinese Academy of Sciences, Hefei 230031, China.

† Electronic Supplementary Information (ESI) available: [Details of experimental procedures, characterization and theoretical calculations]. See DOI: 10.1039/c000000x/

1 R. Niewa, H. Jacobs, *Chem. Rev.*, 1996, **96**, 2053.
2 M. Shalom, V. Molinari, D. Esposito, G. Clavel, D. Ressnig, C. Giordano, M. Antonietti, *Adv. Mater.*, 2014, **26**, 1272.
3 D. Choi, G. E. Blomgren, P. N. Kumta, *Adv. Mater.*, 2006, **18**, 1178.
4 T. He, Q. Huang, A. P. Ramirea, Y. Wang, K. A. Regan, N. Rogado, M. A. Hayward, M. K. Haas, J. S. Slusky, K. Inumara, H. W. Zandbergen, N. P. Ong, R. J. Cava, *Nature*, 2001, **411**, 54.
5 T. Takayama, K. Kuwano, D. Hirai, Y. Kutsura, A. Yamamoto, H. Tkagi, *Phys. Rev. Lett.*, 2012, **108**, 237001.
6 A. Houben, P. Muller, J. V. Appen, H. Lueken, R. Niewa, R. Dronskowski, *Angew. Chem. Int. Ed.*, 2005, **44**, 7212.
7 S. Likubo, K. Kodama, K. Takenaka, H. Takagi, M. Takigawa, S. Shamoto, *Phys. Rev. Lett.* 2008, **101**, 205901.
8 H. S. Lee, D. J. Jang, H. J. Lee, S. I. Lee, S. M. Choi, C. J. Kim, *Adv. Mater.*, 2006, **19**, 1807.
9 D. P. Young, M. Moldovan, D. D. Craig, P. W. Adams, Phys. Rev. B, 2003, 68, 020501.
10 H. Rosner, R. Weht, M. D. Johannes, W. E. Pickett, E. Tosatti, *Phys. Rev. Lett.*, 2001, **88**, 027001.
11 D. J. Singh, I. I. Mazin, *Phys. Rev. B*, 2001, **64**, 140507.
12 H. M. Luo, H. Y. Wang, Z. X. Bi, D. M. Feldman, Y. Q. Wang, A. K. Burrell, T. M. McCleskey, E. Bauer, M. E. Hawley, Q. X. Jia, *J. Am. Chem.* Soc., 2008, **130**, 15224.
13 G. Zou, M. Jain, H. Zhou, H. Luo, S. Baily, L. Civale, E. Bauer, T. McCleskey, A. Burrell and Q. X. Jia, *Chem. Commun.*, 2008, 6022.
14 Y. Y. Zhang, N. Haberkorn, F. Ronning, H. Y. Wang, N. A. Mara, M. J. Zhuo, L. Chen, J. H. Lee, K. J. Blackmore, E. Bauer, A. K. Burrell, T. M. McCleskey, M. E. Hawley, R. K. Schulze, L. Civate, T. Tajima, Q. X. Jia, *J. Am. Chem. Soc.*, 2011, **133**, 20735.
15 H. M. Luo, Y. Lin, H. Y. Wang, J. H. Lee, N. A. Suvorova, A. H. Mueller, A. K. Burrell, T. M. McCleskey, E. Bauer, I. O. Usov, M. E. Hawley, T. G. Holesinger, Q. X. Jia, *Adv. Mater.*, 2009, **21**, 193.
16 B. He, C. Dong, L. H. Yang, X. C. Chen, L. H. Ge, L. B. Mu, Y. G. Shi, *Supercond. Sci. Technol*. 2013, **26**, 125015.
17 R. Al-Merey, J. Karajou, H. Issa, *Appl. Radiat. Isotopes*, 2005, **62**, 501.
18 M. Affronte, J. Marcus, C. Escribe-Filippini, *Solid State Commun.*, 1993, **85**, 501.
19 S. Y. Li, R. Fan, X. H. Chen, C. H. Wang, W. Q. Mo, K. Q. Ruan, Y. M. Xiong, X. G. Luo, H. T. Zhang, L. Li, Z. Sun, L. Z. Cao, *Phys. Rev. B*, 2011, **64**, 132505.
20 H. M. Luo, H. Y. Wang, Z. Bi, G. F. Zou, T. M. McCleskey, A. K. Burrell, E. Bauer, M. E. Hawley, Y. Wang, Q. X. Jia, *Angew. Chem. Int. Ed.*, 2009, **48**, 1490.
21 P. A. Lee, T. V. Ramakrishnan, *Rev. Mod. Phys.*, 1985, **57**, 287.
22 N. R. Werthamar, E. Helfand, P. C. Hohenberg, *Phys. Rev.*, 1966, **147**, 295.
23 D. P. Hampshire, *Handbook of Superconducting Materials*, edited by Cardwell, D. (IOP, Bristol, 2002).

